Phase Relationships, Transparency, and Conductivity in the Cadmium Indate−Cadmium Stannate System

D. R. Kammler and T. O. Mason*

Department of Materials Science and Engineering and Materials Research Center, Northwestern University, Evanston, Illinois 60208

K. R. Poeppelmeier

Department of Chemistry and Materials Research Center, Northwestern University, Evanston, Illinois 60208

Received February 7, 2000. Revised Manuscript Received April 25, 2000

A novel transparent conducting spinel solid solution $Cd_{1+x}In_{2-2x}Sn_xO_4$ ($0 \le x \le 0.75$ at 1175 °C) between cubic $CdIn_2O_4$ and orthorhombic Cd_2SnO_4 has been discovered. The extent of this solid solution is noteworthy given that bulk phase relations determined in air over the temperature range 800−1175 °C demonstrate that cubic (spinel) Cd_2SnO_4 is metastable. Reduced samples exhibit exceptional four-point dc conductivities exceeding 3500 S/cm ($x = 0.70$). The maximum optical gap estimated from diffuse reflectance spectra is ∼3.0 eV for $0 \le x \le 0.15$. The optical gap shows negligible change with reduction, possibly because of combined Moss−Burstein and band-narrowing effects. Abrupt conductivity increases and optical gap decreases at specific compositions, i.e., $x = 0.4$ and 0.2 respectively, may be indicative of a change in cation distribution between tetrahedral and octahedral sites. Room temperature thermopower measurements indicate the change in conductivity across the solution is a consequence of an increase in carrier density and that mobility remains relatively constant.

Introduction

Transparent conducting oxides (TCOs) constitute a unique class of materials that possess both high transparency throughout the visible spectrum and high electrical conductivity. These materials find application as transparent electrodes in photovoltaics, flat panel displays, de-icers, and electrochromic devices. Their high reflectivity in the IR makes them useful heat reflectors. The present industrial TCO of choice is tin-doped indium oxide (ITO). Thin films of this material have conductivities ranging from 1000 to 5000 S/cm and transparencies between 85 and 90% in the visible region.[1] Next generation photovoltaics will require thinner electrodes to ease processing and increase device performance.[2] TCOs with higher conductivity are needed so that sheet resistance does not decrease when the thickness of the electrode decreases. Increasing the carrier density via chemical doping or reduction can be used to increase the conductivity of TCOs; however, increasing the carrier density will increase the absorption by free carriers.[3] Thus, to maintain high transparency, while increasing conductivity, the mobility of future TCOs must be increased.[4] Reports of high mobility in spinel cadmium stannate (Cd_2SnO_4) films have generated interest in this material and analogous materials, such as spinel cadmium indate ($CdIn_2O_4$) films, as future TCOs.

Smith[5] reported orthorhombic cadmium stannate, Cd_2SnO_4, in his investigation of the $CdO-SnO_2$ system. Nozik[6] first demonstrated the potential of this material as a transparent conductor when he prepared amorphous or partially amorphous films (one film exhibited cubic symmetry) with conductivities exceeding 1300 S/cm, optical gaps as high as 2.85 eV, and mobilities as a high at 100 cm^2/(V-s), which he attributed to an unusually low effective mass. In addition to films, Nozik prepared Cd_2SnO_4 powder above 900 °C in the orthorhombic form described by Smith[5] and below 900° in a cubic form tentatively identified as a spinel.[6] Bulk spinel Cd_2SnO_4 has been prepared via a low-temperature coprecipitation route[7] and by transforming orthorhombic Cd_2SnO_4 to spinel form at high temperatures and pressures.[8] Higher conductivities than those reported by Nozik were obtained by Haacke et al.[9] who prepared

* To whom correspondence should be addressed. E-mail: t-mason@nwu.edu.

(1) Lyman, N. R. Transparent Electronic Conductors. In *Proceedings of the Symposium on Electrochromic materials*; Proceedings of the Electrochemical Society, Hollywood, FL, 1989; Carpenter, M. K., Corrigan, D. A., Eds.; The Electrochemical Society: Pennington, NJ, 1990; p 201.

(2) Kazmerski, L. L. *Renewable Sustainable Energy Rev.* **1997**, *1*, 71.

(3) Coutts, T. J.; Wu, X.; Mulligan, W. P.; Webb, J. M. *J. Electron. Mater.* **1996**, *25*, 935.

(4) Mulligan, W. P.; Coutts, T. J. Measurement of the Effective Mass of Transparent Conducting Films of Cadmium Tin Oxide. In *Flat Panel Display Materials III*; Proceedings of the Mater. Res. Soc. Symp., San Francisco, 1997; Fulks, R., G. P., Slobodin, D., Yuzuriha, T., Eds.; Mater. Res. Soc.: Warrendale, PA, 1997; p 117.

(5) Smith, A. J. *Acta Crystallogr.* **1960**, *13*, 749.

(6) Nozik, A. J. *Phys. Rev. B* **1972**, *6*, 453.

(7) Bowden, M. E. *J. Mater. Sci. Lett.* **1990**, *9*, 735.

(8) Siegel, L. A. *J. Appl. Crystallogr.* **1978**, *11*, 284.

10.1021/cm000101w CCC: $19.00
Published on Web 06/22/2000

thin films that were primarily crystalline spinel Cd_2SnO_4 with conductivities as high as 6700 S/cm. High-quality fully crystalline spinel Cd_2SnO_4 films were later produced by Wu et al.[10] with conductivities as high as 8300 S/cm and optical gaps of 3.70 eV.[11] It was determined that the unusually high mobilities in fully crystallized spinel Cd_2SnO_4 films were a consequence of an unusually long scattering time rather than an unusually low effective mass.[4]

Cadmium indate, $CdIn_2O_4$, has been reported to have the spinel crystal structure in both bulk[12−14] and thin film[10,15] form. Single crystals of $CdIn_2O_4$ were prepared by Shannon[14] and found to have conductivities as high as 2000 S/cm. Wu et al.[10] prepared thin films of $CdIn_2O_4$ having conductivities exceeding 4300 S/cm and mobilities as high as 44 cm^2/V-s. Pisarkiewicz et al.[15] reported an optical gap of 3.2 eV for *mostly* polycrystalline $CdIn_2O_4$ films reactively sputtered from a metallic alloy target. It may be possible to prepare $CdIn_2O_4$ films with optical gaps substantially higher than this if completely phase-pure polycrystalline films were made. This seems likely in light of the fact that the same deposition procedure was used to prepare *mostly* polycrystalline spinel Cd_2SnO_4 films with optical gaps near 3.0 eV[15] while high quality single-phase spinel Cd_2SnO_4 films produced via rf sputtering from an orthorhombic Cd_2SnO_4 target had optical gaps as high as 3.7 eV.[11]

Shannon et al.[14] attempted to dope $CdIn_2O_4$ (substituting Sn^{4+} for In^{3+}) by growing single crystals of spinel $CdIn_{2-x}Sn_xO_4$ from a flux of 2.5 CdO:1.0 SnO_2:0.5 In_2O_3, which he reported to have conductivities of 450 S/cm. Cardile[16] attempted to dope Cd_2SnO_4 with In but reported negligible increase in conductivity. Thus, while attempts to dope Cd_2SnO_4 and $CdIn_2O_4$ with In and Sn, respectively, have been made, no research has been done to determine the existence of a solid solution between these TCOs.

The study of bulk TCOs provides information that is useful to those producing TCO films. Palmer et al.[17] discovered a TCO solid solution $In_{2-2x}Sn_xZn_xO_3$ ($0 \le x \le 0.40$ at 1250 °C) isostructural with In_2O_3 that possesses conductivities between 2600 S/cm ($x = 0.1$) and 800 S/cm ($x = 0.4$) and optical gaps between 3.5 eV ($x = 0.1$) and 2.9 eV ($x = 0.40$). It may be possible to grow high-quality TCO films of the same stoichiometry as this solid solution that are substantially less expensive than ITO films given that indium is expensive compared to zinc and tin. Edwards et al.[18] discovered a new ternary TCO having tetragonal symmetry and stoichiometry $Ga_{3-x}In_{5+x}Sn_2O_{16}$ ($0.2 \le x \le 1.6$) with a conductivity of 375 S/cm (reduced, $x = 0.6$) and optical gap near 3.0 eV. Structural analysis revealed that this TCO was an anion-deficient fluorite derivative like ITO and that its substantially lower conductivity may be related to the absence of one of the cation sites present in ITO.[19] Clearly, such bulk structural knowledge is useful in determining how to design a high-quality TCO.

Studying the bulk-phase relations between orthorhombic Cd_2SnO_4 and $CdIn_2O_4$ may provide some insight in to explaining the high mobility reported for the spinel Cd_2SnO_4 phase. Trends in electrical and optical properties measured on samples prepared at different points along the solution may give insight as to how to engineer novel high mobility TCOs. In this paper we report the solubility limit of this solution, the change in conductivity, thermopower, diffuse reflectance (transmittance), and optical gap (estimated from diffuse reflectance) with composition.

Experimental Procedure

Samples were prepared from In_2O_3, SnO_2, and CdO powders (>99.99% purity cation basis, Aldrich Chemical Co., Inc.). Powders were dried at 400 °C for 24 h. and then stored in a desiccator prior to weighing to eliminate adsorbed water. Preweighed portions of the component powders were ground under acetone in an agate mortar and pestle and pressed in a $^1/_4$ in. die at 150 MPa. The pellets were loaded into a cylindrical alumina crucible and buried in a bed of their constituent powders to limit volatilization and contamination from the crucible. A tightly fitting alumina tube sealed at one end was then lowered around the crucible as an additional barrier to limit volatilization of CdO. Pellets were calcined between 20 and 24 h initially at 1000 °C, quenched in air, reground, and repelletized, and then fired at 1175 °C to complete reaction and increase density. Compositions near a phase boundary required an additional regrinding and firing step to achieve equilibrium. Sintered pellets were reduced for 6 h at 400 °C and cooled to ambient temperature under flowing forming gas (4% H_2, 96% N_2).

Phase purity was established and lattice parameters were obtained by powder Cu K_α X-ray diffraction (XRD) (Rigaku, Danvers, MA). A nickel filter was used to remove the K_β contribution from the diffraction pattern. Powders were scanned in 2θ between 10 and 70° with 0.05° increments for phase analysis and between 50 and 140° with 0.02° increments for lattice parameter determination. Peak locations were determined using Peakfit.[20] The peak locations of an internal silicon standard were used to correct the data for both off-axis displacement error and zero-shift error in the diffractometer prior to obtaining the lattice parameter by the method of least squares using the software package POLSQ.[21]

The four-point dc conductivity of quenched pellets was measured at room temperature in an osmium-tipped (radii = 0.254 mm) four-point probe apparatus (Cascade Microtech, Beaverton, OR) interfaced with constant current supply and voltmeter (m 224 and 195A Keithly, Cleveland, OH). The conductivity was calculated using

$$\sigma = \frac{1}{\rho} = 1/\left[\frac{V}{I} wC\left(\frac{d}{s}\right)F\left(\frac{w}{s}\right)\right] \quad (1)$$

Here σ is the conductivity, ρ is the resistivity, I is the current

(9) Haacke, G.; Mealmaker, W. E.; Siegel, L. A. *Thin Solid Films* **1978**, *55*, 67.
(10) Wu, X.; Coutts, T. J.; Mulligan, W. P. *J. Vac. Sci. Technol. A* **1997**, *15*, 1057−1062.
(11) Mulligan, W. P. A Study of the Fundamental Limits to Electron Mobility in Cadmium Stannate Thin Films. Ph.D. Thesis, Colorado School of Mines, Golden, CO, 1997.
(12) Skribljak, M.; Dasgupta, S.; Biswas, A. B. *Acta Crystallogr.* **1959**, *12*, 1049.
(13) Rasines, I. *Z. Kristallogr.* **1974**, *140*, 410.
(14) Shannon, R. D.; Gillson, J. L.; Bouchard, R. J. *J. Phys. Chem. Solids* **1977**, *38*, 877.
(15) Pisarkiewicz, T.; Zakrzewska, K.; Leja, E. *Thin Solid Films* **1987**, *153*, 479.
(16) Cardile, C. M. *Rev. Solid State Sci.* **1991**, *5*, 31.
(17) Palmer, G. B.; Poeppelmeier, K. R.; Mason, T. O. *Chem. Mater.* **1997**, *9*, 3121.
(18) Edwards, D. D.; Mason, T. O.; Goutenoire, F.; Poeppelmeier, K. R. *Appl. Phys. Lett.* **1997**, *70*, 1706.
(19) Edwards, D. D.; Mason, T. O.; Sinkler, W.; Marks, L. D.; Goutenoire, F.; Poeppelmeier, K. R. *J. Solid State Chem.* **1998**, *140*, 242−250.
(20) Winholz, R. A.; Almer, J. D. *Peakfit*, Fortran Program; Northwestern University: Evanston, IL, 1991.
(21) Keszler, D.; Cahen, D.; Ibers, J. *POLSQ*, Fortran Program; Northwestern University: Evanston, IL, 1984.

passed through the outer probes, V is the potential measured across the inner probes, w is the sample thickness, d is the sample diameter, s is the probe tip spacing (1.016 mm), and C and F are correction factors for finite sample diameter and thickness.[22] Since the percent theoretical density ranged between 50 and 70% for spinel samples (the density of orthorhombic Cd_2SnO_4 was 77% of theoretical) these conductivities were corrected for 3−3 porosity using the symmetric medium equation of McLachlan et al.[23]

Room-temperature thermopower was measured by placing the pellets between two gold foil contacts welded to type S (Pt/Pt 10% Rh) thermocouples. The lower gold contact was in thermal equilibrium with a cylindrical steel slug (2 cm diameter, 2 cm tall) resting on a refractory brick, while the top gold contact was in thermal equilibrium with a 23 W soldering iron. Once hot, the iron was switched off and the thermal gradient across the pellet was allowed to decay. The temperature and voltage gradients (measured across the Pt leads) across the sample were measured as functions of time using a digital multimeter and scanner (Keithly models 195A and 705) interfaced through their IEEE ports to a personal computer used to record the data. Temperature and voltage data taken near thermal equilibrium (i.e., the thermal gradient was less than 20 °C and the average absolute temperature was 60 °C) were used to calculate the slope via least squares from a plot of the voltage gradient as a function of the temperature gradient in accordance with the equation:[24]

$$Q = -\lim_{\Delta T \to 0}(\Delta V/\Delta T) \qquad (2)$$

Voltages were corrected for the thermopower of the Pt as described by Hong et al.[24] using the polynomial of Hwang[25] to calculate the Pt thermopower at each data point.

Optical data were obtained via diffuse reflectance. In a diffuse reflectance experiment, the nonspecular component of reflection (i.e., radiation that has undergone multiple scattering events on different particles and returned to the sample surface) is measured relative to a standard.[26] Measurements on bulk samples provide information that is roughly analogous to transmission measurements on thin films.[26] The transmission edge onset (determined by the intersection of lines drawn through the low transmission region and the sloped portion of the spectra joining the high and low transmission regions) was used to estimate an optical gap. Diffuse reflectance was measured from 200 to 800 nm using a double-beam spectrophotometer with an integrating sphere (Cary 1E with Cary 1/3 attachment, Varian Walnut Creek, CA). Baseline spectra were collected using pressed poly(tetrafluoroethylene) (PTFE) powder compacts (Varian part number 04-101439-00) placed in the sample and reference beams. Data were collected with a scan rate of 600 nm/min, a data interval of 1 nm, an averaging time of 0.1 s, and a signal bandwidth of 3 nm. Pellets were mounted on a blackened sample mask.

Results and Discussion

Figure 1 shows the lattice parameter as a function of x in spinel $Cd_{1+x}In_{2-2x}Sn_xO_4$. It is clear that the lattice parameter follows a linear relationship with x in accordance with Vegard's law. The actual change is less than 0.02 Å across the entire solution range. This small change in lattice constant is a consequence of the similarity in size of the substituting Cd^{2+}, Sn^{4+} cations

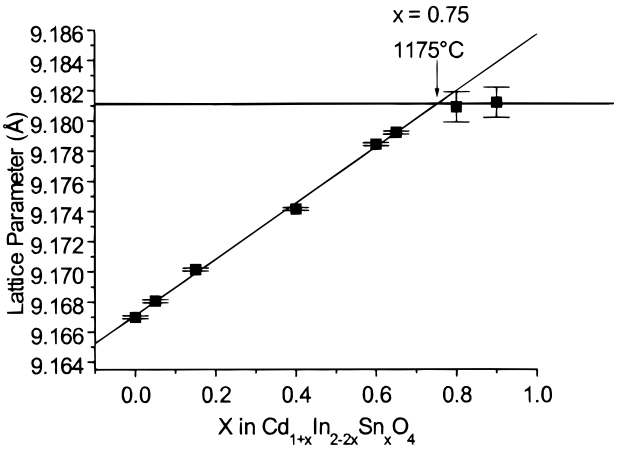

Figure 1. Lattice parameter for $Cd_{1+x}In_{2-2x}Sn_xO_4$ as a function of x at 1175 °C in air. Bulk spinel Cd_2SnO_4 has been prepared with a lattice parameter of 9.177 Å via a low-temperature coprecipitation method[7] and 9.143 Å via a high-temperature and pressure method.[8]

Table 1. Calculated and Experimental Lattice Parameters for $CdIn_2O_4$−Cd_2SnO_4 System[a]

cation distribution	lattice constant (Å)	
	$CdIn_2O_4$	Cd_2SnO_4
normal	9.125	9.183
random	9.105	9.186
inverse	9.092	9.180
measured lattice parameter	9.1670 ± 0.0001	9.1857 ± 0.0001[b]

[a] Calculated lattice parameters are obtained using Shannon's[27] radii and the formulas of O'Neill and Navrotsky.[28] [b] Extrapolated.

to the In^{3+} cation. The octahedral radii as reported by Shannon[27] for Cd^{2+} and Sn^{4+} are 0.95 and 0.69 Å, respectively, while the tetrahedral radii for Cd^{2+} and Sn^{4+} are 0.78 and 0.55 Å, respectively. Thus, the averages of the Sn^{4+} and Cd^{2+} radii are 0.82 and 0.665 Å in octahedral and tetrahedral coordination, respectively. These compare quite closely with 0.80 and 0.62 Å, which are the radii for In^{3+} in octahedral and tetrahedral coordination, respectively.[27] The results of calculations using these radii and equations relating the spinel lattice constant to the cation radii[28] are shown in Table 1 along with experimentally measured lattice constants. The calculated lattice constants predict a much larger change (i.e., at least a factor of 3) than is shown in Figure 1. This observation, which is consistent with the findings of O'Neill and Navrotsky,[28] warrants further study. As can be seen in Figure 1 the solution terminates at $x = 0.75$. The uncertainty of the terminal spinel lattice parameter (determined from biphasic samples) is approximately ±0.001 Å. This leads to an error of ~0.05 (in x) in the phase boundary. Between $x = 0.75$ and 1 both Cd_2SnO_4 (orthorhombic) and the terminal spinel composition coexist. Orthorhombic Cd_2SnO_4 appears to be a line compound. Three samples having the composition corresponding to $x = 0.65$ ($Cd_{1.65}In_{0.70}Sn_{0.65}O_4$) were annealed for 24 h at 900, 1000, and 1100 °C, quenched in air, and then examined to determine whether the lattice parameter had changed. The results of this experiment are shown in Figure 2. The total change was ~0.0004 Å. This is ~50 times less than

(22) Smits, F. M. *Bell Syst. Technol. J.* **1958**, *37*, 711.
(23) McLachlan, D. S.; Blaszkiewicz, M.; Newnham, R. E. *J. Am. Ceram. Soc.* **1990**, *73*, 2187.
(24) Hong, B. S.; Ford, S. J.; Mason, T. O. *Key Eng. Mater.* **1997**, *125*, 163−186.
(25) Hwang, J. Interfacial Electrical/Dielectric Phenomena in Nanoscale Ceramics. Ph.D. Thesis, Northwestern University, Evanston, IL, 1996.
(26) Hecht, H. G. *The Present Status of Diffuse Reflectance Theory*; Wendlandt, W. W., Ed.; Plenum Press: New York, 1968; pp 1−26.
(27) Shannon, R. D. *Acta Crystallogr.* **1976**, *A32*, 751.
(28) O'Neill, H. S. C.; Navrotsky, A. *Am. Mineral.* **1983**, *68*, 181.

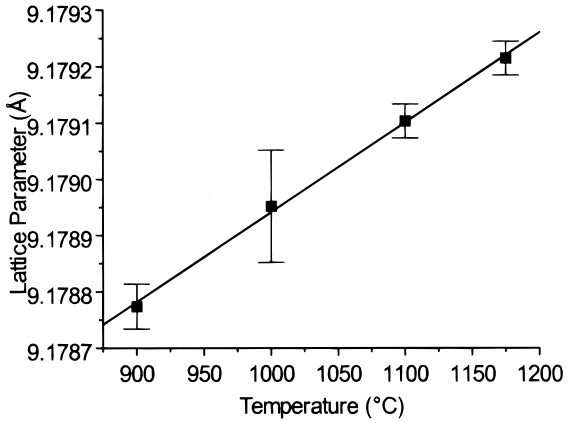

Figure 2. Lattice parameter of $Cd_{1.65}In_{0.70}Sn_{0.65}O_4$ vs temperature in air.

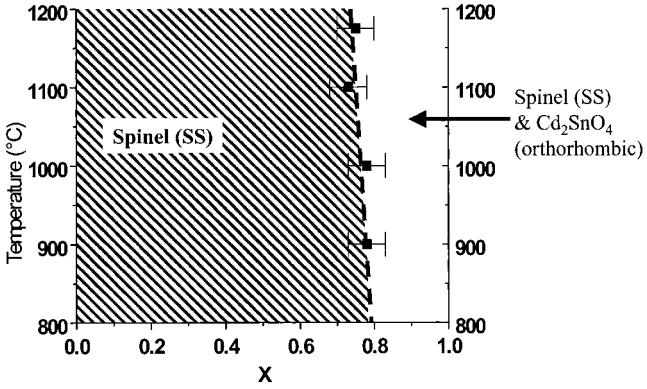

Figure 3. Phase relations for the $(1 - x)$ $CdIn_2O_4$−xCd_2SnO_4 binary in air.

the change measured across the solution in Figure 1. Consequently, it is valid to assume that although the lattice parameter of the line in Figure 1 may not be independent of the annealing temperature, the change is small enough to approximate it as such for purposes of calculating the phase boundary. Thus, the change in the lattice parameter measured for biphasic $x = 0.90$ samples annealed at the same series of temperatures can be used to estimate the change in the phase boundary with temperature. Figure 3 shows a vertical section for the $CdIn_2O_4$−Cd_2SnO_4 system estimated from this change. Although we show a slight decrease in orthorhombic Cd_2SnO_4 solubility with increasing temperature, this is probably not statistically significant, given the uncertainty in the lattice parameter determination, made even more difficult by the large amount of peak overlap owing to the presence of the low symmetry orthorhombic Cd_2SnO_4 phase in the $x = 0.90$ samples.

Figure 4 shows the as-fired and reduced conductivity as a function of x across the solution. Table 2 shows the raw as-fired and reduced conductivity data that were corrected for 3−3 type porosity using the model of McLachlen et al.[23] prior to creating Figure 4. The marked difference in conductivity between the terminal spinel composition and the orthorhombic Cd_2SnO_4 suggests that the high conductivity of the Cd_2SnO_4 films is a consequence of their spinel crystal structure.

Transmitted light optical microscopy was used to confirm transparency on the $x = 0.05$, 0.50, and 0.70 samples. Diffuse reflectance was used to obtain a

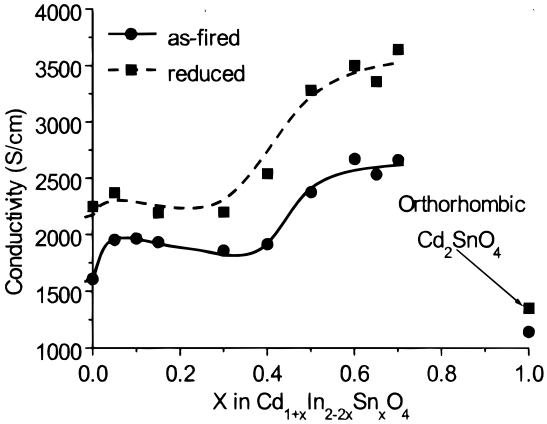

Figure 4. Four-point dc conductivity for as-fired and reduced $Cd_{1+x}In_{2-2x}Sn_xO_4$ as a function of x. Spinel Cd_2SnO_4 films have conductivities as high as 8300 S/cm.[10]

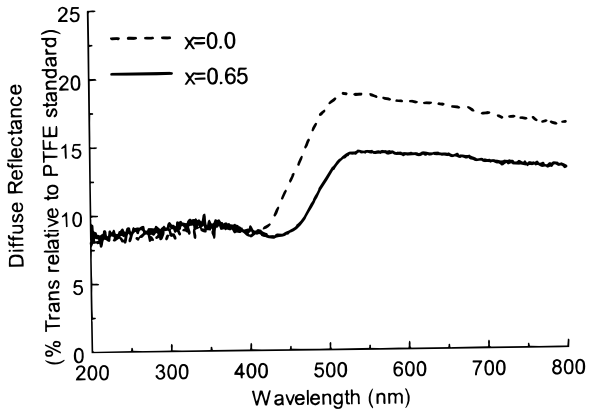

Figure 5. Diffuse reflectance spectra of as-fired $CdIn_2O_4$ ($x = 0$) and $Cd_{1.65}In_{0.7}Sn_{0.65}O_4$ ($x = 0.65$).

Table 2. Conductivity Data Uncorrected for Porosity for As-Fired and Reduced Samples

x in $Cd_{1+x}In_{2-2x}Sn_xO_4$	as−fired conductivity (S/cm)	reduced conductivity (S/cm)
0	546	661
0.05	901	1066
0.1	894	
0.15	891	1037
0.3	796	958
0.4	735	886
0.5	1047	1397
0.6	1444	1915
0.65	1298	1757
0.70	1444	1985
1.0	750	892

measure of the relative transparency of the specimens along the solution in addition to estimating the optical gap of these specimens. Figure 5 shows the diffuse reflectance spectra for as-fired $CdIn_2O_4$ ($x = 0$) and $Cd_{1.65}In_{0.7}Sn_{0.65}O_4$ ($x = 0.65$). The transmission edge onset increases and the diffuse reflectance (transmittance) decreases with x. Figure 6 shows the optical gap for as-fired and reduced specimens prepared along the solution derived from the transmission edge onset of diffuse reflectance spectra like that in Figure 5. It is interesting to note that the increase in conductivity from reduction is not accompanied by a rise in the optical gap (optical gaps shown in Figure 6 have an uncertainty of ~0.1 eV) that one might anticipate from the well-known Moss[29]−Burstein[30] shift. The shift in the Fermi level

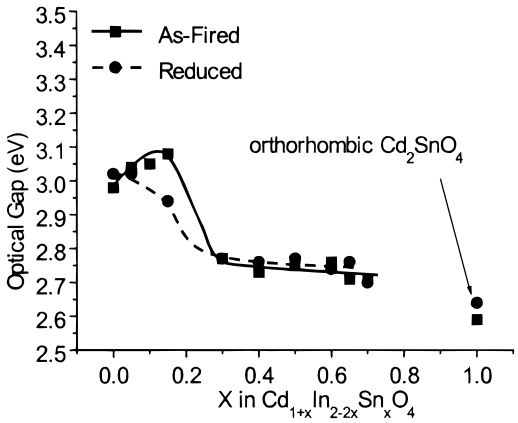

Figure 6. Optical gap estimated from transmission edge onset in diffuse reflectance for as-fired and reduced $Cd_{1+x}In_{2-2x}Sn_xO_4$. Spinel Cd_2SnO_4 films have optical gaps as high as 3.70 eV.[11]

with reference to the conduction band minimum for materials having isotropic parabolic bands is given by the relation:[29]

$$\Delta E_{MB} \propto n^{2/3}/m^* \quad (3)$$

Here n is the carrier density and m^* is the effective mass of the electron. Since the Moss−Burstein shift is a function of both the carrier density and the effective mass of the conduction electron,[29] the absence of an observed shift in optical gap may be a consequence of band bending (i.e., change in effective mass) that counters the increase in carrier density to preserve the ratio in relation 3. This seems unlikely based on the result of Mulligan[11] who determined that the effective mass in spinel Cd_2SnO_4 films remained constant as carrier density changed. While effective mass remains constant with respect to carrier density, substantial band narrowing, owing to electron−electron and electron-impurity scattering that partially offsets the Moss−Burstein shift, has been observed in spinel Cd_2SnO_4 films.[11] Consequently, it seems that the absence of any observed shift in optical gap resulting from reduction shown in Figure 6 is a result of band narrowing that offsets the Moss−Burstein shift.

Figure 7 shows the room-temperature thermopower for reduced samples of $Cd_{1+x}In_{2-2x}Sn_xO_4$ as a function of x. The thermopower for degenerate semiconductors is inversely proportional to the Fermi level according to[31]

$$Q_e \propto T/E_f \quad (4)$$

Here T is temperature and E_f is the Fermi energy. If in addition to being degenerate, the conduction band for $Cd_{1+x}In_{2-2x}Sn_xO_4$ is isotropic and parabolic as assumed previously, then the Fermi energy is given by[11]

$$E_f = (\hbar^2/2m^*)(3\pi^2 n)^{2/3} \quad (5)$$

Here n is the carrier density and m^* is the effective mass. Equation 5 and relation 4 can then be combined so that the change in carrier density along the solution

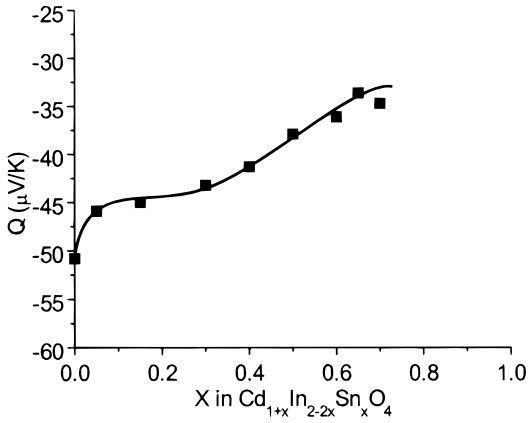

Figure 7. Room temperature thermopower (Q) as a function of x in reduced $Cd_{1+x}In_{2-2x}Sn_xO_4$.

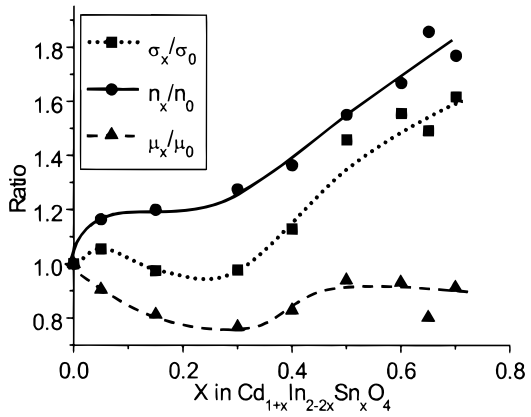

Figure 8. Conductivity (σ), carrier density (n), and mobility (μ) normalized to that of $CdIn_2O_4$ in the solution $Cd_{1+x}In_{2-2x}Sn_xO_4$ as a function of x for reduced samples.

$Cd_{1+x}In_{2-2x}Sn_xO_4$ can be determined from the change in thermopower in Figure 7. This change in carrier density can then be used in combination with the conductivity data in Figure 4 to calculate the change in mobility (with x) across the spinel solution. The carrier density, conductivity, and mobility changes of reduced samples relative to $CdIn_2O_4$ are plotted in Figure 8 as a function of x in $Cd_{1+x}In_{2-2x}Sn_xO_4$. Figure 8 clearly establishes that the change in conductivity in Figure 4 is caused by an increase in carrier density rather than mobility. Consequently, it can be concluded that either the dopant level in the solution is increasing with x or the solution is more readily reduced under the same conditions (i.e., 6 h at 400 °C in 4% H_2/96% N_2) as x increases. In addition, it appears that while control over the stoichiometry in the solution $Cd_{1+x}In_{2-2x}Sn_xO_4$ can be used to vary the dopant level, it is the spinel structure itself that is responsible for the high mobility.

Another interesting feature present in Figures 4 and 6 is an inflection point in each plot. In both as-fired and reduced samples the conductivity rises initially and remains relatively flat until approximately $x = 0.4$, after which it increases rapidly and levels off again near $x = 0.6$. A sudden drop in optical gap in Figure 6 at $x = 0.2$ mirrors the sudden upturn in conductivity in Figure 4. These inflection points in Figures 4 and 6 may be indicative of a change in cation distribution between tetrahedral and octahedral sites. Resolving the cation distribution in the ternary spinel may provide some clue

(29) Moss, T. S. *Proc. Phys. Soc. A.* **1954**, *382*, 775.
(30) Burstein, E. *Phys. Rev.* **1954**, *93*, 632.
(31) Smith, R. A. *Semiconductors*, 1st ed.; Cambridge University Press: Cambridge, 1961.

as to why these inflection points exist and it is therefore the subject of ongoing work. Mössbauer data have been used to show that spinel cadmium stannate films with slightly different Cd/Sn ratios have different Sn s-electron densities that correlate with the conductivity.[32] This may be indicative of a change in cation distribution in the films. Both Cardile[32] and Stapinski[33] determined from the presence of quadrupole splitting in their Mössbauer experiments that Sn^{4+} was octahedrally coordinated in spinel Cd_2SnO_4 films, suggesting an inverse distribution of cations (i.e., half the Cd^{2+} is on tetrahedral sites while the other half of the Cd^{2+} and all the Sn^{4+} are on octahedral sites). While this is consistent with the strong octahedral and tetrahedral preference of Sn^{4+} and Cd^{2+}, respectively,[34] it does not rule out a somewhat random distribution (i.e., some of the Sn^{4+} may sit on tetrahedral sites).

Attempts have also been made to resolve the cation distribution in spinel $CdIn_2O_4$. Skribljak et al.[12] were unable to determine from XRD a favored cation distribution and decided on the inverse case (i.e., 50% of the In^{3+} on the tetrahedral site and the remainder along with the Cd^{2+} on octahedral sites) based on an increased octahedral site preference enthalpy of Cd^{2+} over In^{3+} as calculated by Miller.[35] On the other hand, tetrahedral and octahedral metal-to-oxygen bond lengths calculated from X-ray data suggest that $CdIn_2O_4$ may have a normal distribution of cations (i.e., Cd^{2+} on tetrahedral positions and In^{3+} on octahedral positions).[14] Using 9.115 Å for the lattice parameter and 0.385 for the oxygen position parameter as determined from XRD by Skribljak et al.[12] Shannon et al. calculated a tetrahedral-oxygen bond length of 2.14 Å and an octahedral-oxygen bond distance of 2.19 Å.[14] They noted the $^{IV}Cd^{2+}-^{IV}O^{2-}$ bond distance of 2.14 Å in the normal spinel CdV_2O_4 as measured by Reuter et al.[36] matched the tetrahedral-oxygen bond distance measured in $CdIn_2O_4$.[14] Furthermore, using 0.78, 0.95, 0.62, 0.80, and 1.38 Å as the radii for $^{IV}Cd^{2+}$, $^{VI}Cd^{2+}$, $^{IV}In^{3+}$, $^{VI}In^{3+}$, and $^{IV}O^{2-}$ ions respectively,[27] Shannon et al.[14] concluded that the calculated $^{IV}Cd^{2+}-^{IV}O^{2-}$ bond distance of 2.16 Å compares more closely to the measured tetrahedral-oxygen bond distance of 2.14 Å than the calculated $^{IV}In^{3+}-^{IV}O^{2-}$ bond distance of 2.00 Å and the calculated $^{VI}In^{3+}-^{IV}O^{2-}$ bond distance of 2.18 Å compares more closely to the measured octahedral-oxygen bond distance of 2.19 Å than the calculated $^{VI}Cd^{2+}-^{IV}O^{2-}$ bond distance of 2.33 Å.

This argument depends critically on the accuracy of the radii for the Cd^{2+} and In^{3+} cations in the different coordination environments and the accuracy of the measured lattice parameter and oxygen position parameter. O'Neill and Navrotsky[28] found slight differences between a number Shannon's general (i.e., averaged over a large number of *different* crystal structures) ionic radii and a set of their own tailored to match structural data from a large number of *spinels* (unfortunately, no corrections for $^{VI}Cd^{2+}$, $^{IV}Sn^{4+}$, $^{IV}In^{3+}$, $^{VI}In^{3+}$ are given). Furthermore, as previously mentioned, the smaller than expected change in lattice constant observed in Figure 1 could reflect problems in the use of ionic radii or have some other physical explanation. For example, modeling Cd^{2+}, In^{3+}, and Sn^{4+} as hard spheres in the spinel structure may yield lattice constants with an uncertainty in the first decimal place. O'Neill and Navrotsky[28] noted that many of the published oxygen position parameters may be in error given the difficulty of determining them. Even a small error in the oxygen position parameter will greatly affect the octahedral and tetrahedral bond distances (e.g., an identical lattice parameter of 9.115 Å and a u of 0.378 would give a tetrahedral-oxygen bond distance of 2.02 Å and an octahedral-oxygen bond distance of 2.25 Å, which might lead one to conclude $CdIn_2O_4$ had an inverse distribution of cations).

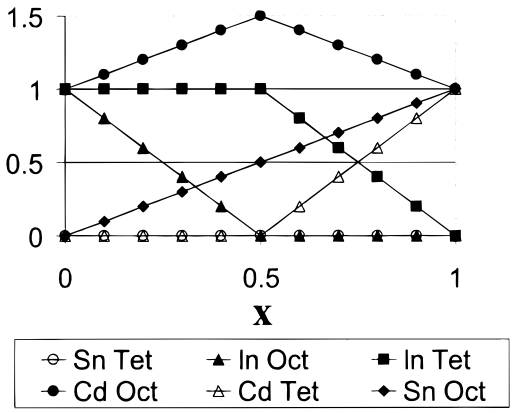

Figure 9. Site distribution in $Cd_{1+x}In_{2-2x}Sn_xO_4$ as a function of x assuming both Cd_2SnO_4 and $CdIn_2O_4$ have an inverse cation distribution and that Cd^{2+} has a greater octahedral site preference enthalpy than In^{3+}.

While the cation distribution in $CdIn_2O_4$ is unclear, it is still possible to speculate how the site distribution changes throughout the ternary solution if one concludes from ^{119}Sn Mössbauer studies[32,33] that Cd_2SnO_4 is an inverse spinel. If $CdIn_2O_4$ is also an inverse spinel, owing to an increased octahedral site preference of Cd^{2+} over In^{3+} as concluded by Skribljak et al.,[12] then the model presented in Figure 9 might apply. In this case In^{3+} remains on the tetrahedral position until the exact center of the solution ($x = 0.5$) while one Cd^{2+} and one Sn^{4+} replace two In^{3+} on the octahedral position. Thereafter, two In^{3+} cations on tetrahedral sites are both displaced by two Cd^{2+} cations, one of which was displaced from a neighboring octahedral site by a substituting Sn^{4+} ion. If on the other hand $CdIn_2O_4$ has a normal distribution as proposed by Shannon et al.[14] the model shown in Figure 10 might apply. Now Cd^{2+} remains on the tetrahedral position throughout the solution while all the substitution takes place on the octahedral sublattice (i.e., two In^{3+} cations are replaced by one Cd^{2+} and one Sn^{4+} cation).

A comparison of the conductivity data in Figure 4 and the cation distribution in Figure 9 reveals a correlation between the onset of Cd^{2+} tetrahedral occupancy at $x = 0.5$ in Figure 9 and the upturn in conductivity at $x = 0.4$. If the difference in octahedral site preference enthalpy of the Cd^{2+} and In^{3+} is small enough, configurational entropy effects may allow intermixing of Cd^{2+} and In^{3+} on the tetrahedral site below $x = 0.5$. This

(32) Cardile, C. M.; Koplick, A. J.; McPherson, R.; West, B. O. *J. Mater. Sci. Lett.* **1989**, *8*, 370.
(33) Stapinski, T.; Japa, E.; Zukrowski, J. *Phys. Status Solidi A* **1987**, *103*, K93.
(34) Navrotsky, A.; Kleppa, O. J. *J. Inorg. Nucl. Chem.* **1967**, *29*, 2701.
(35) Miller, A. *J. Appl. Phys.* **1959**, *30*, 24S.
(36) Reuter, V. B.; Riedel, E.; Hug, v. P.; Arndt, D.; Geisler, U.; Behnke, J. *Z. Anorg. Allg. Chem.* **1969**, *369*, 306.

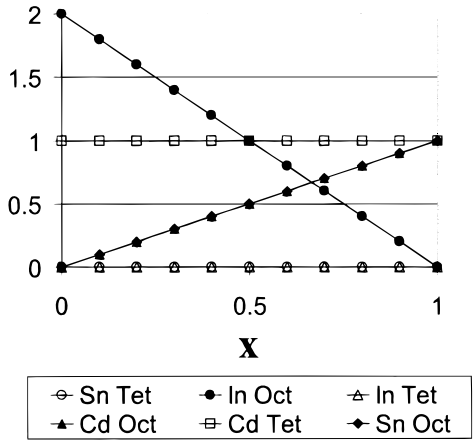

Figure 10. Site distribution in $Cd_{1+x}In_{2-2x}Sn_xO_4$ as a function of x assuming Cd_2SnO_4 and $CdIn_2O_4$ have inverse and normal cation distributions respectively and that In^{3+} has a greater octahedral site preference enthalpy than Cd^{2+}.

might explain why the onset of the conductivity increase in Figure 4 occurs slightly before $x = 0.5$ (i.e., at $x = 0.4$). There is no analogous change in site distribution at $x = 0.20$ in either Figures 9 or 10, the point where the optical gap shows a marked decrease in Figure 6. Clearly more work needs to be done to determine whether the conductivity increase and/or the optical gap decrease correlate with changes in site distribution of cations.

Neutron diffraction should resolve the cation distribution in $CdIn_2O_4$ and $Cd_{1+x}In_{2-2x}Sn_xO_4$ (using a suitable isotope such as ^{112}Cd in place of naturally occurring Cd) since Cd^{2+}, In^{3+}, and Sn^{4+} have different scattering factors for neutrons (they have identical X-ray scattering factors).[37] In addition, O^{2-} scatters neutrons more strongly than X-rays[37] and could therefore be used to obtain a more accurate estimate of the oxygen position parameter and the oxygen−metal bond distances. Such experiments are ongoing and will be reported separately.

If the exact end-member distributions can be obtained, the distributions in intermediate compositions can be estimated. A thermodynamic model proposed by O'Neill and Navrotsky[28,38] estimates site preference enthalpies from the end-member distributions that can then be used to model the changes in cation distribution across the ternary solution. With experimental confirmation these distributions may provide a deeper understanding of TCO behavior in this solution.

One important ramification of this study is the apparent metastability of the spinel form of Cd_2SnO_4. Whereas the bulk spinel solid solution terminates between $x = 0.75$ and 0.8 in $Cd_{1+x}In_{2-2x}Sn_xO_4$ over the temperature range 800−1175 °C, beyond which the orthorhombic form of Cd_2SnO_4 becomes the stable phase, it is well-known that thin films of pure Cd_2SnO_4 ($x = 1$) grown at much lower temperatures readily crystallize in the spinel form. It is unlikely that the slope of the phase boundary in Figure 3 can account for this. Given the subtle lattice parameter vs composition relationship in Figure 1, however, it is quite possible that surface area and/or substrate-induced strain effects in thin films facilitate the formation of the metastable spinel phase.

Conclusions

The phase relationships in the $CdIn_2O_4$−Cd_2SnO_4 system were investigated in air over the temperature range 800 °C to 1175 °C. The $(1 - x)CdIn_2O_4$−xCd_2SnO_4 spinel solid solution was shown to extend from $x = 0$ to approximately $x = 0.75$ at 1175 °C. Between $x = 0.75$ and $x = 1$, the spinel phase is in equilibrium with essentially pure orthorhombic Cd_2SnO_4. The solubility limit of orthorhombic Cd_2SnO_4 in the solid solution may increase slightly as temperature decreases; however, the trend is insufficient to account for the tendency of pure Cd_2SnO_4 thin films to crystallize in the spinel form.

The electrical conductivity and optical transparency of the $(1 - x)CdIn_2O_4$−xCd_2SnO_4 solid solution were measured at room temperature on as-fired and reduced (forming gas annealed) specimens. The conductivity of reduced specimens varies between approximately 2000 S/cm for $x = 0$ to in excess of 3500 S/cm for the terminal composition ($x \approx 0.75$). In comparison, the orthorhombic form of Cd_2SnO_4 has significantly lower conductivity (∼1300 S/cm) in the reduced state. Optical gap in the solid solution, as determined by diffuse reflectance measurements, varies from 3.0 eV at $x = 0$ to 2.7 eV at $x \approx 0.75$. Both properties (conductivity, optical gap) exhibit sharp changes—conductivity rises sharply (at $x = 0.4$) and optical gap drops precipitously (at $x = 0.2$). Room temperature thermopower data from reduced specimens indicate the conductivity increase can be attributed to an increase in carrier density and that the mobility appears to be a constant for this solution. These changes may signal a change in cation distribution that needs to be better understood to optimize the transparent conducting behavior of this solid solution.

Acknowledgment. This work was supported in part by the MRSEC program of the National Science Foundation (DMR-9632472) at the Materials Research Center of Northwestern University and by the Department of Energy through the National Renewable Energy Laboratory under subcontract number AAD-9-18668-05. The central facilities of the Materials Research Center were used extensively in the research. Dan Kammler was supported by a National Science Foundation Graduate Fellowship.

CM000101W

(37) Wilson, A. J. C.; Ed. *International Tables for Crystallography*, 3rd ed.; Kluwer Academic Publishers: Boston, 1992; Vol. C.
(38) O'Neill, H. S. C.; Navrotsky, A. *Am. Mineral.* **1984**, *69*, 733.